ARTICLE IN PRESS

ELSEVIER

Journal of Nuclear Materials 307–311 (2002) 843–851

journal of nuclear materials

www.elsevier.com/locate/jnucmat

Section 10. Fundamentals of defects and radiation effects in materials

Mechanisms of dislocation-defect interactions in irradiated metals investigated by computer simulations

N.M. Ghoniem [a,*], S.H. Tong [a], J. Huang [a], B.N. Singh [b], M. Wen [a]

[a] *Department of Mechanical and Aerospace Engineering, University of California, 46-147G Engr. IV, UCLA, 420 Westwood Plaza, Los Angeles, CA 90095-1597, USA*

[b] *Department of Materials Research, RISØ National Laboratory, DK-4000 Roskilde, Denmark*

Abstract

During irradiation, mobile defects, defect clusters and impurity atoms segregate on dislocations. When an external stress is applied, plastic flow is initiated when dislocations are unlocked from segregated defects. Sustained plasticity is achieved by continuation of dislocation motion, overcoming local forces due to dispersed defects and impurities. The phenomena of flow localization, post-yield hardening or softening and jerky flow are controlled by dislocation-defect interactions. We review here computational methods for investigations of the dynamics of dislocation-defect interactions. The influence of dislocations on the motion of glissile self-interstitial atoms (SIAs) and their clusters is explored by a combination of kinetic Monte Carlo and dislocation dynamics. We show that dislocation decoration by SIAs is a result of their 1-D motion and rotation as they approach dislocation cores. The interaction between dislocations and immobilized SIA clusters indicates that the unlocking mechanism is dictated by shape instabilities. Finally, computer simulations for the interaction between freed dislocations and stacking fault tetrahedra in irradiated Cu, and between dislocations and microvoids in irradiated iron are presented, and the results show good agreement with experimental observations.

1. Introduction

Metal deformation in response to external forces is well-established to be a result of dislocation generation and motion. While the onset of plastic yield is correlated with the *initiation* of dislocation motion, subsequent hardening or softening are clearly controlled by the *continuation* of such motion. Plastic yield and subsequent hardening (or softening) are primarily determined by the mechanisms that control dislocation motion. In unirradiated metals, dislocation–dislocation interactions play a very significant role in determining the characteristics of plastic deformation, where the impedance of dislocation motion is associated with the formation of sessile junctions or dipoles. In body centered crystals (bcc), however, the flow stress and the presence of an upper yield point can be drastically changed by small additions of impurities. Also, in some alloyed fcc metals (e.g. copper crystals containing zinc), the upper yield point has also been observed. To explain this effect, Cottrell [1] showed that the flow stress at the upper yield point is a consequence of dislocation detrapping from impurity *clouds*, which are attracted to dislocations because of their elastic interaction with dislocations. In an irradiation environment, however, neutron collisions with lattice atoms produce copious densities of intrinsic defects, thus reducing or inhibiting dislocation motion in response to external forces. The initiation of plastic yield in irradiated metals is therefore almost entirely controlled by dislocation interaction with intrinsic defects.

The general features of the stress–strain curve of irradiated pure fcc metals are similar to those of unirradiated bcc metals containing impurities. At some critical

* Corresponding author. Tel.: +1-310 825 4866; fax: +1-310 206 4830.

E-mail address: ghoniem@ucla.edu (N.M. Ghoniem).

0022-3115/02/$ - see front matter
PII: S0022-3115(02)01092-9

irradiation dose (e.g. ~0.1 dpa in Cu), an upper yield point emerges, followed by a drop in the yield strength. Most dislocations are observed to be heavily *decorated* by small, sessile interstitial clusters [2]. To explain the experimentally observed yield drop, and to understand the relationship between dislocation decoration and the yield behavior of irradiated materials, the *cascade induced source hardening* (CISH) model has been proposed (see Refs. [2–4]). In this concept, self-interstitial atom (SIA) defect cluster mobility and trapping in the stress field of grown-in dislocations are assumed to be the main reason behind experimental observations of dislocation decoration, and the corresponding presence of an upper yield point in irradiated fcc metals and alloys. Decorations of dislocations in irradiated fcc metals indicate the presence of sessile interstitial dislocation loops produced by coalescence of mobile SIA clusters outside a *stand-off* distance from the dislocation core. Mobile SIA clusters that approach the dislocation at closer distances are absorbed into the dislocation core [3,5]. On the basis of this picture, the CISH model was used to estimate the flow stress of irradiated metals as the stress necessary to *unlock* dislocations from immobile SIA coagulated clusters. In this model, however, as in Kropua's analysis of similar hardening problems [6], dislocations are assumed to be rigid during their interaction with defects.

Once dislocations are released from localized SIA clusters, they will undoubtedly move very fast under the same applied stress that unlocked them, and unless their motion is further hindered, strain softening may occur. In irradiated fcc metals, dislocation motion past the initial yield point is determined by *additional* interactions with lattice defects in the form of sessile stacking fault tetrahedra (SFTs) or Frank vacancy loops. On the other hand, it is found that a high density of microvoids in bcc metals control the post-yield hardening or softening behavior in irradiated bcc metals [7]. The overriding theme here is that the phenomena of yield initiation, emergence of an upper yield point in fcc metals, the magnitude of radiation hardening (i.e. increase in CRSS), the subsequent hardening or softening, the formation of microslip bands (i.e. dislocation channels), and eventual fracture of irradiated materials are all dictated by the details of dislocation-defect interactions. The companion overview article [7] addresses the relationships between dislocation-defect interaction and experimental observations on radiation hardening, yield drop, and post-yield plasticity of irradiated bcc and fcc metals. The main objective of the present work, however, is to focus on the computational and mechanistic aspects of dislocation-defect interactions in irradiated materials. The specific goal of the present work is to utilize large-scale computational simulations to explore the mechanisms by which dislocation motion is impeded in irradiated materials. First, we discuss how dislocations are decorated, trapped and detrapped by SIA defect clusters. We then determine the mechanisms of dislocation-defect interactions during subsequent deformation in irradiated materials. To understand the formation of microshear bands (dislocation channels) in irradiated materials, a full simulation for the dynamics of dislocation motion and interactions *within* dislocation channels in both fcc (e.g. Cu) and bcc (e.g. Fe) will be presented. Also, the effects of microvoids on dislocation channel formation in irradiated Fe will be discussed.

2. Brief review of computational methods

2.1. Parametric dislocation dynamics

Since it was first introduced in the mid-eighties [9,10], dislocation dynamics (DD) has now become an attractive and effective tool for investigations of both fundamental and collective processes that constitute plastic deformation of crystalline materials. Recently, Ghoniem and coworkers [11–15] have shown that if dislocation loops are discretized into curved parametric segments, one can obtain the field by numerical integration over a scalar parameter that represents the segment. Once the parametric curve for the dislocation segment is mapped onto the scalar interval $\{\omega \in [0,1]\}$, the stress field everywhere is obtained as a fast numerical quadrature sum [11]. The Peach–Kohler force is then obtained on any other segment point as: $\mathbf{F}_{\mathrm{PK}} = \sigma \cdot \mathbf{b} \times \mathbf{t}$. The self-force is obtained from knowledge of the local curvature at the point of interest. The variational form of the governing equation of motion (EOM) of a single dislocation loop is given by: $\int_\Gamma (F_k^t - B_{\alpha k} V_\alpha)\delta r_k |\mathrm{d}\mathbf{s}| = 0$. Here, F_k^t are the components of the resultant force, consisting of the Peach–Koehler force $\mathbf{F}_{\mathrm{PK}}$ (generated by the sum of the external and internal stress fields), the self-force $\mathbf{F}_{\mathrm{s}}$, and the osmotic force $\mathbf{F}_{\mathrm{O}}$ [12]. The resistivity matrix (inverse mobility) is $B_{\alpha k}$, V_α are the velocity vector components, and the line integral is carried along the arc length of the dislocation d$\mathbf{s}$ [12].

2.2. Kinetic Monte Carlo for defect motion in stress fields

In performing KMC simulations, we follow an approach introduced by Bortz et al. [16], which ensures that one event occurs somewhere in the system, and that the time increment itself can be determined at each step. In this approach, since one event occurs at each simulation step and different events occur at different rates, the time increment, dt, corresponding with each step is dynamic and stochastic: $\mathrm{d}t = -\ln(\xi)/\sum_{i=1}^{M} r_i$, where ξ is a random number. This method is particularly useful in simulations of radiation-induced defect motion, where the events occur at vastly different time scales.

So far, all KMC computer simulations for microstructure evolution under irradiation have not considered the influence of the internal and applied stress fields on defect motion. We present here computer simulations, where the elastic interactions between SIA clusters themselves, and between SIA clusters and dislocations are explicitly accounted for. SIA clusters are directly produced on the periphery of neutron collision cascades, and they may contain from a few atoms up to tens of atoms in the near vicinity of the cascade [17]. Such clusters are extremely mobile, and migrate predominantly along highly packed crystallographic directions, with migration energies of less than 0.1 eV [17,18]. Small SIA clusters may also spontaneously change their Burgers vector, and thus have the flexibility to translate along various crystallographic directions if their motion is not obstructed by internal strain fields. In this work, we represent SIA clusters as small prismatic, rigid and circular dislocation loops.

The temperature dependence of the jump frequency of SIA cluster diffusion can be written as follows:

$$\omega = \omega_0 \exp\left(-\frac{E_m}{kT}\right),$$

where ω is the cluster jump frequency, ω_0 the pre-exponential factor, E_m the migration energy in a perfect crystal structure, T the temperature of the crystal and k the Boltzmann constant. In our KMC simulations, the elastic interaction is considered. The influence of other defects and the external stress on one SIA cluster is given by the stress field σ_{ij}. The work necessary to form the loop characterized by normal $\mathbf{n}$, Burgers vector $\mathbf{b}$ and area δA in the stress field σ_{ij} is SIA cluster interaction energy E_{int}, and is given by [6]

$$E_{int} = n_i b_j \sigma_{ij} \delta A = \mathbf{n} \cdot \sigma \cdot \mathbf{b}.$$

The total cluster migration energy is then given by

$$\widetilde{E}_m = E_m + \Delta E_{int},$$

where ΔE_{int} is the change in the interaction energy of an SIA cluster placed at two neighboring equivalent points in the crystal. This includes the effects of forces and moments on the virtual loop motion. It has been shown that small SIA clusters can form perfect loops and perform one-dimensional (1-D) random motion in the slip direction [17–19]. There is a total of eight equivalent $\langle 1\,1\,1\rangle$ slip directions for SIA clusters in bcc Fe. Thus, there are eight equivalent choices for each cluster at each KMC step. However, the restriction of diffusion to 1-D motion implies that the possibility of reorientation for an SIA cluster is rather small, and the migration energy of a preferred $\langle 1\,1\,1\rangle$ direction is much lower than that of all other seven equivalent directions. We use the frequency of a loop jumping along a $\langle 1\,1\,1\rangle$ orientation, ω, as the rate at which an event occurs in our KMC model. Therefore, there is a total of $8N$ possible events for the N SIA clusters at each KMC step.

3. Dislocation interaction with glissile defect clusters

During irradiation, mobile SIA clusters migrate very quickly, interact with other features of the microstructure or amongst themselves, and they become immobilized as a consequence of such interactions. If they end up near the core of grown-in dislocations, they form what is known as a cluster atmosphere, similar to the well-known Cottrell impurity atmosphere around dislocations in unirradiated bcc metals. The yield behavior of the material is thus expected to be heavily dependent on the local cluster density near the dislocation core, and on how dislocations interact with such clusters. First, we present a study of cluster motion under the influence of the internal stress field created by grown-in dislocations as well as the clusters themselves. In post-irradiation tensile tests, dislocation unlocking from immobilized clusters controls the magnitude of the initial plastic yield (i.e. the upper yield stress), and thus, we will present computer simulations for the unlocking process also in this section.

3.1. Dislocation decoration

To study how glissile SIA clusters migrate and interact amongst themselves, and with internal stress fields generated by dislocations and applied mechanical loads, a computational box of $400a \times 400a \times 400a$ (a: lattice constant of bcc Fe) is used with periodic boundary conditions. A uniaxial tensile stress of 121 MPa is applied along the $\langle 1\,0\,0\rangle$ direction. In order to study dislocation-cluster interaction, a dislocation loop lying on the $\langle 0\,\bar{1}\,1\rangle$ plane, with Burgers vector $\frac{1}{2}\langle \bar{1}\,1\,1\rangle$ is introduced into the simulation box. The loop is generated by using the parametric method described above. The dislocation loop consists of two curved segments and two straight junction segments that are normal to the loop's Burgers vector. An initial number of SIA clusters with the same size (1.7 nm diameter) are first randomly distributed in the simulation cell, and their initial jump directions are also randomly specified. The SIA cluster density is varied in the range 5×10^{22}–2×10^{23} M^{-3}. The orientation of each cluster's Burgers vector is kept the same as the jump direction, because clusters are represented as small prismatic dislocation loops. When a cluster approaches the dislocation loop at distances closer than the *stand-off* distance (taken as 1.5 nm), the cluster is stopped, and all the events related to it are removed from the event table. The code allows cluster coalescence when two clusters overlap with one another. In the present KMC simulations, we use the following

input parameters for bcc Fe: Migration Energy $E_m = 0.02$ eV, lattice constant $a = 2.8665$ Å, initial cluster radius $R = 3$ (a), Temperature $T = 300$ K, pre-exponential factor $\omega_0 = 2.5 \times 10^{13}$, ratio of migration energy of 1-D motion relative to reorientation energy $f = 7.0$, shear modulus $\mu = 81.8$ GPa, and Poisson's ratio $v = 0.29$.

Computer simulations of cluster–cluster-dislocation interactions reveal a number of interesting features. First, the migration of SIA clusters is very fast, and within a few nano-seconds at room temperature, clusters migrate along highly packed crystallographic directions over microstructurally significant distances. Previous MD simulations of motion of isolated SIA clusters indicated that their migration along $\{1\,1\,1\}$ in bcc metals is extremely fast, as a result of their very low migration energies (~0.02 eV) [20]. It is expected that the overall transport of SIA clusters is dependent on their density, and on their interaction with other strain centers in the crystal. The present KMC simulations reveal that their mutual elastic interactions at the high level of concentrations brings about a drastic decrease in their long-range transport. Their mutual interaction fields, aided by the focusing effects of internal dislocation fields, renders these clusters virtually immobile just after a few nano-seconds, as can be seen in Fig. 1. In effect, these clusters re-orient themselves by rotation of their Burgers vector to respond to the elastic field of internal dislocations. Thus, their migration is *focused* towards internal stress fields, and not random, as implied by MD simulations. Moreover, because of their close proximity, which is induced by the tendency to crowd space in the vicinity of dislocations, their mutual interaction becomes very strong. Clusters that are oriented along non-parallel crystallographic orientations will either coalesce forming larger ones, or just pin one another at a short distance and become immobile. Another interesting feature of this problem is that when clusters are within a distance of several nano-meters from each other, and have their Burgers vectors in parallel directions, will trap one another and tend to move in a self-organized group or *raft*. This feature has been experimentally observed for some time [7].

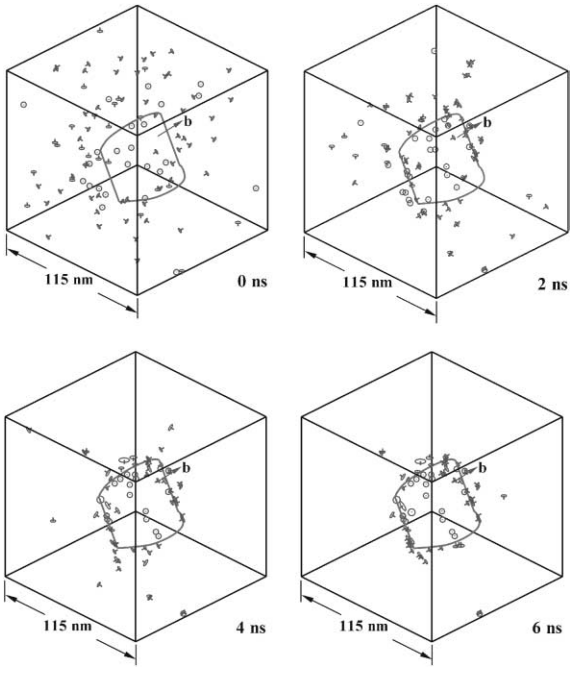

Fig. 1. KMC simulation of SIA diffusion and clustering in the stress field of a 3-D dislocation loop. Self-assembled SIA loop *rafts* are clearly observed on lower left corner, and close to edge orientations of the loop.

4. Dislocation interaction with sessile defect clusters

Nano-scale precipitates, SFTs and small voids are all sessile in irradiated materials, and one can assume that their force field is localized at a point on the glide plane. Because of the large density and the numerous interactions of such obstacles to dislocation motion, dislocation loops are parametrically represented as small circular arcs inscribed in between obstacle points on the glide plane [21].

The total number of obstacles (e.g. precipitates, vacancy clusters and SFTs) are calculated from their experimentally measured densities and the simulation cube size. The percentage of destructible obstacles (e.g. SFTs or vacancy clusters) is also specified. Each loop segment is represented by a circular arc, and its curvature is determined by the applied stress, sum of all interaction forces, and Burgers vector. When a loop segment encounters the nearest obstacle, it splits into two segments and each segment continues to move until it reaches its equilibrium curvature, or when the angle between the two tangents at the obstacle reaches a critical value, Φ_c. A kinetic Monte Carlo (KMC) procedure is implemented to determine the probability of obstacle destruction (for SFTs and microvoids), or the dislocation cutting through the obstacle (for precipitates). The probability of cutting/destruction is calculated from the height of the energy barrier, the work done by the local forces at tangent points, and the lattice temperature. Once an event has been determined, the *waiting time* t_w is calculated by the KMC method described in the previous section, and the obstacle is either destroyed or cut-through. After annihilation, these two segments merge into one and the unified segment is advanced till it meets the next obstacle on the plane, and the corresponding free flight time t_f is also recorded. The total advance time between obstacles is the sum of these two, i.e. $t_a = t_w + t_f$. The procedure is repeated for all segments, and a

general time clock records the corresponding time for the evolution of the dislocation loop shape.

When a vacancy cluster or microvoid is destroyed, the vacancy contents are assumed to be absorbed immediately into the dislocation core in between two obstacles, and a climb distance is obtained from the number of vacancies contained in the obstacle divided by the segment length. An expanding dislocation loop will then have segments on different, parallel glide planes. When the segment climbs and jumps to another parallel plane, the intersections between obstacles and the new plane are calculated and used for finding new interactions on that plane. The properties of every obstacle in 3-D are tracked by array variables, which store integer numbers representing different properties. Once an obstacle (SFT or microvoid) is destroyed, it is immediately detected by tracking the corresponding array variable.

Periodic boundary conditions are implemented for the expansion of loops emanating from Frank–Read sources. The distance between each segment and the nearest boundary is calculated with every time step. Once a segment is detected to be out of the simulation boundaries, a different integer is assigned to the array variables, and the segment motion is continued from the boundary at the opposite side, and the segment is placed on a parallel glide plane. The distance between any two segments from the same dislocation loop (F–R source) is calculated to determine if it is less than a prescribed length (about the half of average segment length). The two closest segments are then determined, and annihilation is implemented. The old loop will then be split at these two segments and re-connected to the segment on the other side. This process involves the generation of a new open loop with two pinned ends (F–R source), and the majority of the old loop becomes an expanding closed loop. All properties from the old loop are also assigned to the new open loop in order that it can continue its motion. The interaction forces between segments are calculated every time step because they are used to determine the segment curvature. The free flight time t_f for a segment is measured from an initial straight segment in between two obstacles to the curved configuration, where the segment touches the nearest obstacle. Therefore, the free flight time is determined by the curvature and segment length. The waiting time is measured from the time an obstacle is contacted till its cutting or annihilation.

4.1. Interaction with stacking fault tetrahedra in fcc metals

Once dislocations are freed from their locking defect cluster atmospheres, they will move on their glide planes till they encounter other obstacles to their motion. The yield drop at this moment is associated with a sudden increase in the plastic strain originating from released dislocations, thus requiring a drop in the applied stress to maintain a constant rate of total strain. The post-yield behavior of irradiated fcc specimens is determined by dislocation interaction with sessile vacancy clusters, which can be either SFT type, or vacancy loop type. Here, we consider the case of irradiated annealed copper at room temperature. The experimentally measured values of SFT density and size are given in Table 1 below.

Fig. 2 shows the results of computer simulations for the expansion of dislocation loops generated from Frank–Read sources on [1 1 1]-glide planes in Cu under incrementally increasing applied stress. The resistance of SFTs to the expansion of dislocations from F–R sources requires an increase in the applied stress to maintain a constant rate of strain. Thus, on active glide planes, a *local* stress–strain diagram can be obtained, as seen in Fig. 2, where the results are shown for four different irradiation doses. The macroscopic stress–strain curve, however, cannot be precisely determined unless one knows the fraction of active slip volumes within the tested sample; a task beyond the capabilities of current simulations. Following the yield drop, the lower yield point can be predicted by computer simulations for the interaction between released dislocations and SFTs that intersect glide planes. Fig. 3 shows a direct comparison between experimentally measured values for the increase in the yield strength and those calculated by computer simulations as a function of the irradiation dose. The only adjustable parameter in these calculations is the critical angle for destruction of a single SFT, which is

Table 1
Experimentally measured SFT density, size and hardening ($\Delta\sigma_{exp}$) in annealed Cu [22], and calculated results for different critical angles

Case	Dose	$\Delta\sigma_{exp}$ (MPa)	SFT density ($\times 10^{-23}$ M^{-3})	SFT size (nm)	Calculated $\Delta\sigma$		
					$\Phi_c = 160°$	$\Phi_c = 165°$	$\Phi_c = 170°$
1	0.01	38	0.45	3.0	71	39	31
2	0.1	105	1.4	4.5	120	105	80
3	0.2	115	1.7	4.5	145	115	100
4	0.3	120	2.5	4.0	155	125	110

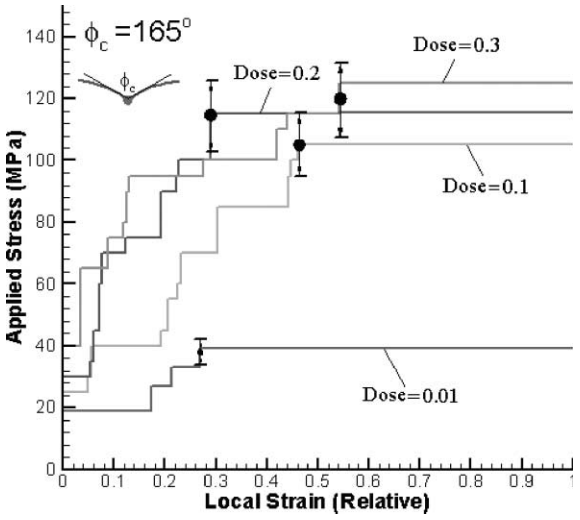

Fig. 2. Local stress–strain diagrams at different doses for annealed Cu irradiated at 100 °C.

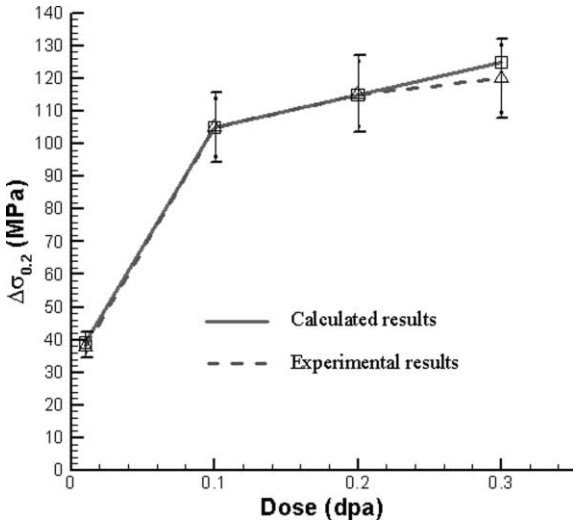

Fig. 3. A comparison between results of computer simulations and experimental data for annealed Cu irradiated at 100 °C.

found to be $\Phi_c = 165°$ for optimum correspondence between experiment and computer simulations. Table 1 shows the sensitivity of the results of computer simulations to variations in the value of the critical angle, Φ_c.

4.2. Interaction with microvoids in bcc metals

In irradiated bcc metals, vacancies generated by collision cascades form small voids, while interstitials are carried away from cascade centers in SIA clusters. Therefore, dislocations that are released from SIA cluster atmospheres will interact with dispersed voids in the matrix in a similar fashion to the situation in fcc metals, where dislocations interact with SFTs or vacancy loops. Under the action of an applied stress, dislocations impinge on nano-size voids and may destroy them if the work done by local forces exerted by dislocations on microvoids exceeds a critical value determined by the elastic interaction energy. In the present computer simulations, we *assume* that the small nano-size void is destroyed by the dislocation, once the angle between the arms of the dislocation that surround the void exceeds a critical value, Φ_c. Thus, Φ_c is viewed as the only adjustable parameter here, and its value can be precisely calculated through molecular dynamics (MD) computer simulations [8]. It is important, however, to determine the *energy* of dislocation cutting through voids rather than Φ_c in MD simulations, and then convert that energy into the corresponding Φ_c by the elastic point force model.

Fig. 4 shows the results of computer simulations for the stages of dislocation channel evolution in irradiated Fe. The model parameters are given in Table 2 below. Initially, dislocations in a local area of stress concentration or statistically low SIA cluster atmosphere density are activated when the local shear stress reaches a critical value. In Fig. 4(a), one such F–R source is activated at a stress level of 30 MPa. When the applied stress is increased to 65 MPa (Fig. 4(b)), several F–R sources are shown to have their dislocations bowing out in response to the applied stress and mutual interaction forces. However, only a few have expanded significantly to reach the edge of the simulation cube. Also shown in the same figure is the pre-annihilation stage of one of the F–R source dislocations, where two segments are about to annihilate, thus creating a full loop and restoring the initial pinned dislocation segment of the source. In Fig. 4(c), further activation of dormant F–R sources is achieved, when the local microvoid density is effectively reduced by the passage of nearby dislocations. A *domino* effect is thus created, where the destruction of microvoids in a local region by one source activates other nearby sources. It is to be noted that the dislocation loop structure is not planar, because of the continuous climb process associated with each dislocation glide event. At a stress level of 70 MPa, dislocation loops start to impinge on the simulation box boundary, and at that point, periodic boundary conditions are implemented to inject those loop segments that emerge from one side of the boundary to the other side, as can be seen in Fig. 4(d) and (e). The evolution process is terminated when the leading-edge loop reaches the grain boundary or surface (which is assumed here to be 10 μm), and successive dislocation loops interact with one another to form a non-planar pileup of loops that would exert sufficient

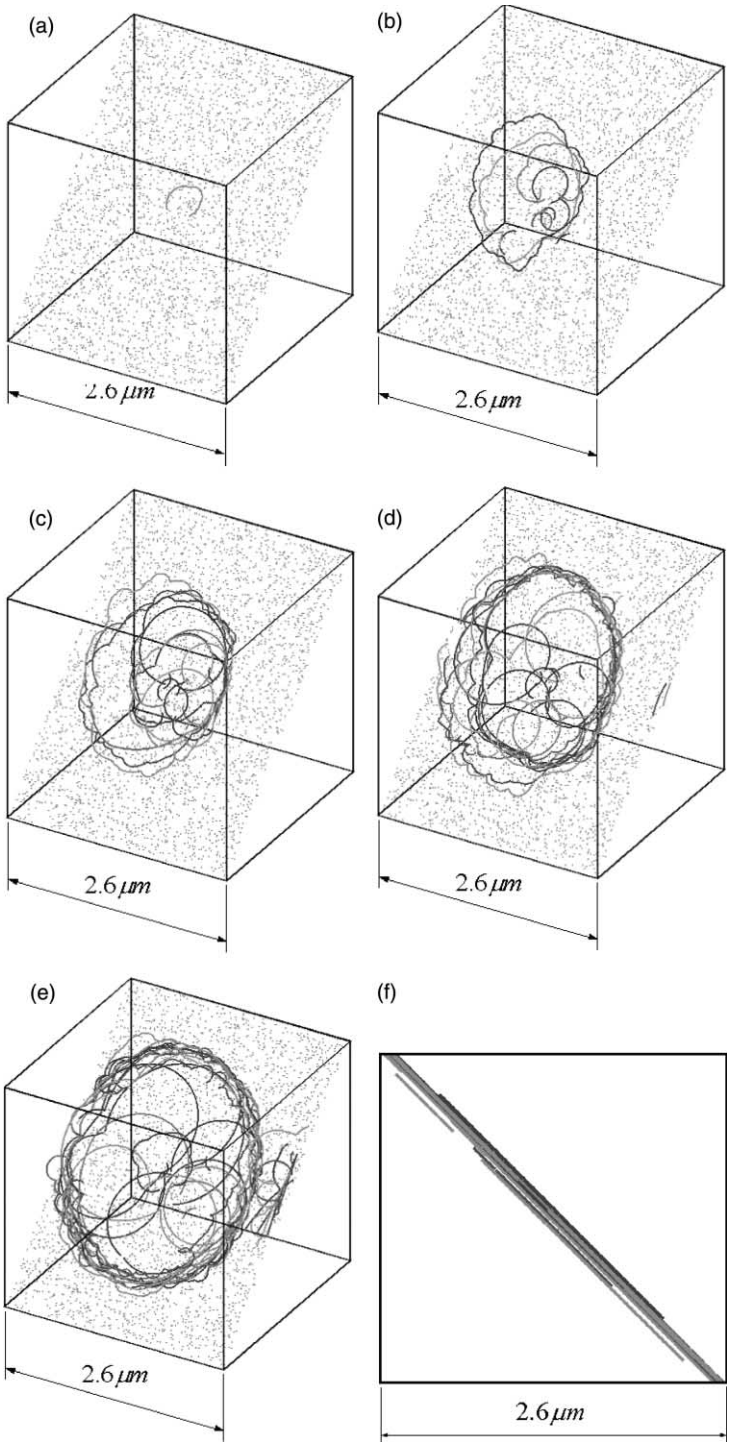

Fig. 4. Various stages for the development of a dislocation channel in irradiated Fe. (a)–(e) shows the evolution of dislocation loops as they interact amongst themselves and microvoids on planes parallel to $\{1\,0\,1\}$-planes, while (f) shows the dislocation channel edge-on (the $\langle 0\,\bar{1}\,0\rangle$)-direction is towards the viewer.

back stress on all sources to shut them off. The structure of the evolving non-planar pileup of loops is shown from the side view (the $\langle 0\,\bar{1}\,0\rangle$-direction is towards the viewer) in Fig. 4(f).

Table 2
Input parameters for the computer simulations of Fig. 4 for irradiated Fe

Dose (dpa)	σ_{exp} (MPa)	Void density ($\times 10^{-23}$ M^{-3})	Void size (nm)	Simulation size (μm) cube	Number of F–R sources	Grain size (μm)
0.01	65	0.5	0.6	2.6	10	10

5. Conclusions and future outlook

The main theme of the present overview is to delineate how large-scale computer simulations of dislocation-defect interactions in irradiated materials can reveal physical insights that can be used to construct either simpler analytical models, or help in experimental design. The ultimate objective of computer simulations is to be useful in designing radiation-resistant alloys, once the basic mechanisms are clearly determined. This task is not complete, however, unless the results of computer simulations are compared to specific experiments that are designed to test the validity of the mechanisms themselves. In this article, we have shown that large-scale computer simulations provide insight that cannot be gained from analytical theory or experiments alone, but once all aspects are considered, one is more certain of the nature of investigated mechanisms. In a companion article [7], the emphasis is shifted towards the question of how one can use experimental observations to drive more realistic computer models. We conclude here that the current methods of computer simulations of dislocation defect interactions, namely, the DD and KMC techniques used separately and in combination, have resulted in defining a clearer picture of how SIA clusters attract to dislocations to decorate and lock them in place, how they form rafts and how they pin themselves and not move around at vast speeds. It also resulted in understanding the fundamental mechanism of dislocation unlocking from defect cluster atmospheres, where dislocations pull themselves out of such atmospheres by reconfiguration and shape instabilities. Finally, the basic mechanisms of radiation hardening beyond the upper yield point, and the ensuing nucleation and propagation of *dislocation channels* have been demonstrated by large-scale computer simulations. The agreement with experimental observations of radiation hardening has been demonstrated with only one adjustable parameter. In addition, correspondence between TEM observations on dislocation decoration, raft formation and dimensions of dislocation channels has been shown, and is fully discussed in Ref. [7].

Future efforts are expected to address a number of yet un-resolved issues in the area of radiation embrittlement and plastic instabilities. These are:

1. Computer simulations of entire grains, coupling DD with the more macroscopic crystal plasticity models, where lattice rotations, load transfer, and dislocation interaction with boundaries may determine the spacings observed in between dislocation channels;
2. An emphasis on *materials design* aspects, where one would integrate computer models of alloyed materials with experimental design to understand how plastic flow can be managed over larger volumes to delay or retard dislocation channel formation and fracture;
3. Utilization of computer simulations to design new experiments, which would reveal the synergistic effects of applied stress and irradiation on material deformation.

Acknowledgements

Research is supported by the US Department of Energy (DOE), Office of Fusion Energy Sciences (OFES), through grants DE-FG03-00ER54594 and DE-FG03-01ER54626 with UCLA, and is partially funded by the European Fusion Technology program.

References

[1] A.H. Cottrell, Report of Conference on the Strength of Solids, University of Bristol, England, Physical Society, London 30 (1948) 30.
[2] B.N. Singh, A.J.E. Foreman, H. Trinkaus, J. Nucl. Mater. 249 (1997) 103.
[3] H. Trinkaus, B.N. Singh, A.J.E. Foreman, J. Nucl. Mater. 249 (1997) 91.
[4] H. Trinkaus, B.N. Singh, A.J.E. Foreman, J. Nucl. Mater. 251 (1997) 172.
[5] N.M. Ghoniem, B.N. Singh, L.Z. Sun, T. Diaz de la Rubia, J. Nucl. Mater. 276 (2000) 166.
[6] F. Kroupa, Czech. J. Phys. B 10 (1960) 284.
[7] B.N. Singh, N.M. Ghoniem, H. Trinkaus, these Proceedings.
[8] Yu.N. Osetsky, D.J. Bacon, B.N. Singh, B. Wirth, these Proceedings.
[9] J. Lepinoux, L.P. Kubin, Scripta Met. 21 (1987) 833.
[10] N.M. Ghoniem, R. Amodeo, Solid State Phen. 3&4 (1988) 377.
[11] N.M. Ghoniem, L.Z. Sun, Phys. Rev. B 60 (1) (1999) 1.
[12] N.M. Ghoniem, S.-H. Tong, L.Z. Sun, Phys. Rev. B 61 (2000) 913.
[13] N.M. Ghoniem, J. Eng. Mater. Tech. 121 (2) (1999) 136.
[14] N.M. Ghoniem, J.M. Huang, J. Phys. (Paris) IV 11 (5) (2001) 53.
[15] N.M. Ghoniem, J. Huang, Z. Wang, Philos. Mag. Lett. 82 (2) (2002).

[16] A.B. Bortz, M.H. Kalos, J.L. Lebowitz, J. Comp. Phys. 17 (1) (1975) 10.
[17] Yu.N. Osetsky, A. Serra, V. Priego, MRS Symp. Proc. 527 (1998) 59.
[18] N. Soneda, T. Diaz De La Rubia, Philos. Mag. A 78 (1998) 995.
[19] Yu.N. Osetsky, D.J. Bacon, A. Serra, Philos. Mag. Lett. 79 (1999) 273.
[20] Yu.N. Osetsky, D.J. Bacon, A. Serra, B.N. Singh, S.I. Golubov, J. Nucl. Mater. 276 (2000) 65.
[21] N.M. Ghoniem, S.H. Tong, B.N. Singh, L.Z. Sun, Philos. Mag. A 81 (11) (2001) 2743.
[22] B.N. Singh, D.J. Edwards, P. Toft, RISØ National Laboratory Report, No. RISØ-R-1213(EN), February 2001, pp. 30;
J. Nucl. Mater. 299 (2001) 205.